

DRAFT

Next Generation Adaptive Optics Preliminary Design Wavefront Error Budgets

Richard Dekany, COO

April 6, 2010

Abstract

The purpose of this note is to summarize the wavefront error and encircled energy budgets for the Next-Generation Adaptive Optics (NGAO) system at the time of the NGAO Preliminary Design Review.

These budgets are based upon a set of architecture design choices and functional requirements flowdowns consistent with the NGAO System Requirements, which are maintained in an online Requirements Management database product, Contour, developed by JAMA Software, Inc. and commercially licensed by W.M. Keck Observatory.

Revision Sheet

Release No.	Date	Revision Description
Rev. 0.1	4/5/10	Initial draft by R. Dekany
Rev 0.2	4/6/10	Added Gal Assembly Ensquared Energy curves, NGS WFS TWFS mode TT error vs. guide star mag, histogram comps to Keck 2 AO, and more text to prior sections.

Table of Contents

<i>Abstract</i>	1
<i>Revision Sheet</i>	1
1 Introduction	4
1.1 Acronyms and Definitions	4
1.2 Purpose	4
1.3 Scope	4
1.4 Related Documents	4
Configuration-Controlled Documents.....	4
Previous NGAO Performance Documents.....	5
Keck AO Performance Analyses.....	5
References.....	5
2 NGAO Performance Requirements	5
3 Architectural and Observational Elements	6
4 Science Case Parameters	8
5 Detailed Error Budget for Galaxy Assembly Key Science Case	10
5.1 Science Path Wavefront Error Budget	10
5.2 TT Sharpening Budget	11
5.3 TWFS Budget	11
6 LGS Mode operation with 5 x 5 subaperture NGS WFS TWFS mode	12
6.1 Describe the mode of operation	12
6.2 Performance Estimate	12
7 Trade Studies	13
7.1 Performance vs. Seeing	13
7.2 Performance vs. Wind Speed	14
7.3 Performance vs. Laser Return	14
7.4 Seeing, Wind Speed, and Sodium Abundance Monte Carlo Results	16
7.5 Performance vs. Sky Fraction	19
7.6 Performance vs. LO WFS Passband	19
7.7 Performance vs. Spaxel Sampling	20
<i>Appendix A: System Compliance Matrix</i>	<i>21</i>
<i>Appendix B: Wavefront Error Budget Spreadsheet v2.0</i>	<i>22</i>
<i>Appendix C: Detailed Error Budgets</i>	<i>24</i>
Input Summary	24

Galactic Center Case	25
ExoPlanet.....	26

1 Introduction

1.1 Acronyms and Definitions

DAVINCI	A new science instrument under development as part of NGAO
d-IFU	Deployable IFU
EncE	Encircled Energy
EnsqrE	Ensquared Energy
FoV	Field of View (the field observed by a single detector array)
FoR	Field of Regard (the technical or patrol range of a sensor)
FWHM	Full-Width at Half-Maximum = 2.355σ , for a Gaussian distribution
HOWFS	High-order wavefront sensor
IFU or IFS	Integral Field (Unit) Spectrograph
LGS	Laser Guide Star
LO WFS	Low-Order Wavefront Sensor
mas	Milliarcseconds
NGAO	Next-Generation Adaptive Optics
NGS	Natural Guide Star
NGWFC	Next-Generation Wavefront Controller
PSF	Point Spread Function
RMS	Root Mean-Squared
TT	Tip-tilt
TWFS	Truth Wavefront Sensor
WCS	Well-corrected subaperture.
WFE	Wavefront reconstruction error
"	arcseconds
'	arcminutes

1.2 Purpose

The purpose of this document is to document the assumptions, architecture choices, performance flowdown requirements, and expected wavefront error and encircled energy performance for the NGAO science cases.

1.3 Scope

This document includes all defined NGAO science case error budgets, sample TT sharpening budgets, and several trade studies performed to capture NGAO performance.

1.4 Related Documents

Configuration-Controlled Documents

- KAON 550, NGAO System Configurations
- KAON 636, Observing Operations Concept Document
- KAON 721, Wavefront Error Budget Tool

- KAON 722, NGAO High-Contrast Error Budget Tool
- KAON 723, Performance Flowdown Budgets

Previous NGAO Performance Documents

- KAON 452, MOAO versus MCAO Trade Study Report
- KAON 465, NGAO LGS Wavefront Sensor: Type and Number of Subapertures Trade Study
- KAON 470, NGAO Sky Coverage Modeling
- KAON 471, NGAO Wavefront Error and Ensquared Energy Budgets (for System Design Phase)
- KAON 475, Tomography Codes Comparison and Validation for NGAO
- KAON 480, Astrometry for NGAO
- KAON 492, NGAO Null-Mode and Quadratic Mode Tomography Error
- KAON 497, NGAO High-Contrast and Companion Sensitivity Performance Budget
- KAON 503, Mauna Kea Ridge Turbulence Models
- KAON 504, NGAO Performance vs. Technical Field of View for LOWFS Guide Stars
- KAON 594, Plan to Address Phased Implementation and Descope Options
- KAON 601, NGAO Point and Shoot (SPIE 2008)
- KAON 621, Noise Propagator for Laser Tomography AO
- KAON 629, Error Budget Comparison with NFIRAOS
- KAON 635, Point & Shoot Study
- KAON 644, Build-to-Cost Architecture Performance Analysis
- KAON 710, Latency, Bandwidth, and Control Loop Residual Relationships

Keck AO Performance Analyses

- KAON 461, Wavefront Error Budget Predictions & Measured Performance for Current & Upgraded Keck AO
- KAON 462, NGAO Trade Study: Keck AO Upgrade
- KAON 469, Effect of Keck Segment Figure Errors on Keck AO Performance
- KAON 482, Keck Telescope Wavefront Error Trade Study
- KAON 500, Keck AO Upgrade Feasibility

References

- CIN 626, PALM-3000 Error Budget Summary
- J. W. Hardy, *Adaptive Optics for Astronomical Telescopes* (Oxford U. Press, 1998).
- KAON 416, Atmospheric Sodium Density from Keck LGS Photometry
- KAON 477, Modeling Low Order Aberrations in Laser Guide Star AO Systems (OE 2007)
- KAON 478, Modeling Laser Guide Star Aberrations (OSA 2007)
- KAON 574, Systems Engineering Management Plan
- KAON 583, Work Breakdown Structure Definitions

2 NGAO Performance Requirements

The highest-level performance requirements for NGAO are documented in the Systems Requirements section of the NGAO Requirements Contour Database (see Appendix A), with the key requirement for wavefront and ensquared energy documented in SR-20, summarized in Table 1.

NGAO Key Science Case	High-order RMS Wavefront Error (nm)	RMS TT Error (mas)	Effective Total RMS Wavefront Error (nm)	Ensquared Energy within a 70 mas spaxel	Observing Passband	Typical Single-Integration Time (sec)
Galaxy Assembly	163	4.9	185	74	K	1800
Nearby AGN's	163	4.7	181	26 w/in 34 mas	Z	900
Galactic Center	190	2.2	193	59	H	10
Exoplanets	162	3.8	174	68	H	300
Minor Planets	164	4.7	181	25	K	120
Io	115	2.1	117	83	K	10

Table 1. High-level NGAO Performance Requirements Summary from SR-20.

During the NGAO design phases, there has been a close iterative process of feedback between the technical and science teams to determine the best science return obtainable, particularly in light of the Build-to-Cost project decision documented in KAON 642. For reference the historical transition of the performance requirements, including current Keck AO Performance as documented in KAON 461, is shown in Table 2. In general, cost reductions have resulted in the performance degradation of some science cases (typically reflecting the loss of the wide-field d-IFU capability) and the performance enhancement of others.

3 Architectural and Observational Elements

The NGAO WFE budgets are developed using a common WFE budget Microsoft Excel spreadsheet tool developed at Caltech by R. Dekany and collaborators over the past 10 years. It has been extensively validated against other budgets (Wizinowich, Neyman, van Dam, others), detailed Monte Carlo simulations (Arroyo, LAOS), and across projects (see KAON 629 for one example). Fundamentally, it allows selection of an adaptive optics system configuration (such as Keck 2 AO, Keck 1 AO, or NGAO), a Science Case (such as Galaxy Assembly, Io, T Tauri objects, etc.), and a science instrument (such as DAVINCI, OSIRIS, PHARO, etc.) The architectural and observational differences between these choices are almost entirely captured on a single ‘Input Parameters’ worksheet of the workbook. The selection of WFS camera frame rates and offaxis NGS brightnesses and distances are typically optimized parameters that are found subject to constraints of necessary sky coverage fraction or guide star brightness, in the case of a known specific science target. Thus, each error budget for NGAO corresponding to each key science case, assumes operation at a slightly different frame rate¹.

¹ A future revision to KAON 721 may support definable, selectable WFS frame rates, but this is not currently supported.

Error budgets are summarized on the ‘Optim’ worksheet, as this is location of the optimization parameters. (Optim is commonly used for the generation of trade study results, as well.) Separate error budgets are maintained for the science path, the sharpening of field TT stars, and for the wavefront error residual sensed by the TWFS (if applicable). For patrolling LGS TT sharpening systems, the camera frame rates of corresponding HO LGS WFS’s are separately optimized. Additional description of this tool is provided in Appendix C.

NGAO Key Science Case	2006 Keck 2 AO Performance in 75 th Percentile Best Seeing (approx.)	Expected Keck 1 AO Performance in Median Seeing (approx.)	NGAO Requirements in Median Seeing			
			Proposal ^{2,3}	SDR	B2C	Current (PDR)
Galaxy Assembly	557 ⁴	529 ⁵	197 ⁶	257	204	185
Nearby AGN's	557 ⁴	529 ⁵	197 ⁶	N/A	182	181 ⁷
Galactic Center	N/A	387 ⁸	182	184	189	193
Exoplanets	378 ⁹	311 ¹⁰	N/A	155 ¹⁰	171	174
Minor Planets	557 ⁴	529 ⁵	131	175	177	181 ¹¹
Io	258 ¹²	210 ¹³	125	148 ¹³	N/A	117

Table 2. Progression of AO Performance Requirements to Date (N/A = Not available).

² Slight revisions to the Key Science Cases have been made during PD phase. See McGrath and Max, “Science Case Parameters for Performance Budgets” for more details.

³ June 20, 2006 NGAO Design and Development Proposal, Table 13.

⁴ KAON 461, Table 1 for LGS mode with 18th magnitude TT star.

⁵ KAON 461, Appendix 3 for LGS mode with 18th magnitude TT star.

⁶ June 20, 2006 NGAO Design and Development Proposal, Figure 49, for 30% sky coverage, z = 30 deg, having 173 nm HO error and

⁷ Performance increase driven by reduced FoR for this science case brought on by Build-to-Cost decision to eliminate a d-IFU instrument from the NGAO program.

⁸ Jessica Lu, private communication, who reports NGWFC median performance of 401 nm RMS. Here, we assume Keck 1 LGS will provide the same improvement as shown in KAON 461, Table 2, for LGS with 10th magnitude TT star, namely the subtraction of 105 nm in quadrature, so $\sqrt{401^2 - 105^2} = 387$ nm.

⁹ KAON 461, Table 1 for LGS mode with 10th magnitude TT star.

¹⁰ KAON 461, Appendix 2 for LGS mode with 10th magnitude TT star.

¹¹ Performance decrease driven primarily by simplification to laser asterism and reduction in laser power.

¹² KAON 461, Table 1 for NGS ‘bright star’ performance.

¹³ KAON 461, Appendix 1 for NGS mode with 8th magnitude TT star. Note, NGWFC should have similar performance, as the Keck 1 LGS upgrade will not affect NGS science performance.

The NGAO system architecture choices are documented in the configuration region of the Input Summary tab of the Wavefront Error Budget Tool, KAON 721. The key elements of this table are summarized in Table 5. Not shown here, but a critical to budget fidelity is an area of the Input Summary that selects optical pass-bands for each WFS camera. (Also not shown are optical transmission models that track expected photon transmission through each AO system configuration.)

4 Science Case Parameters

Science Case parameters for NGAO have been updated by Max and McGrath during the NGAO preliminary design phase. The updated parameters are shown for convenience in Table 3.

Science Case Name	Zenith Angle (Deg)	Guide stars	NGS color	Required sky coverage (%)	Galactic latitude, b (deg)	Science Filter	Evaluation Filter	Max Single Exposure Time (Sec)	LGS/NGS	NGAO Key Science Case	Applicable to NGAO (Yes/No)
Galaxy Assembly, e.g. Extended Groth	30	Field Stars	M	30	≥60	Z, J, H, K	K	1800	LGS	Y	Key Science Driver
Nearby AGNs	30	Field Stars	M	30	≤60	Z, J, K	Z	900	LGS	Y	Key Science Driver
Galactic Center	50	IRS 7, 9, 12N	N/A	N/A	N/A	H, K	H	<10 (image) 900 (spectra)	LGS	Y	Key Science Driver
Exo-planets	30	Field Stars	M	30	≤30	J, H	H	300	LGS	Y	Key Science Driver
Minor Planets	30	Field Stars	M	30	≤60	Z	Z	120	LGS	Y	Key Science Driver
Io	30	Science Object	G	N/A	N/A	H	H	10	NGS	N	
Vesta	30	Science Object	G	N/A	N/A	J, Z, J, H, K	I'	10 (image) 30 (spectra)	NGS	N	
Exo Jupiter NGS	30	Science Object	M	N/A	N/A	H	H	2 ??	NGS	N	
MIRA Vars	30	Science Object	M	N/A	30	H	H	2	NGS	N	
Faint NGS	10	Science Object	K	N/A	30	K	K	30	NGS	N	
T Tauri	30	Field Stars	M	N/A	N/A	K	K	300	LGS	N	Science Driver
Transients	30	Field Stars	M	30	40	Z, J, H, K	Z	900	LGS	N	Science Driver
Astrometry	30	Field Stars	M	30	40	H	H	30?	LGS	N	Science Driver
Debris Disk	30	Field Stars	M	N/A	20	I', Z	I'	300	LGS	N	Science Driver

Table 3. Science Cases Parameters for NGAO PD phase.

The performance summary of the NGAO PD phase design for all these Science Cases is summarized in Table 4.

XXX Need to compile the full performance matrix for all the science cases in Table 3. XXX

Table 4. Summary of NGAO Science Case Performance.

Input Parameter Summary					
Model		Performance Summary			
AO System	NGAO LGS	HO Error	163 nm		
Science Case	Galaxy Assembly	TT Angular Error	4.9 mas		
Instrument	DAVINCI	Total Effective Error	185 nm		
x					
Worksheet	Parameter	Current Parameter Value	Units	Galaxy Assembly	NGAO LGS
Telescope	Name	Keck		Keck	
Atm	Declination				20
	Zenith Angle	30.0	deg	30	
	Cn2(h) Model	Mauna Kea Ridge		Mauna Kea Ridge	0.160
	r0 at Zenith	0.160	m		9.5
	Wind speed	9.5	m/s		50
	Outer Scale	50	m		
HO Flux	Guide Star Spectral Type	LGS	(NGS/LGS)	LGS	
	Guide Star Brightness	LGS	mV		
	HOWFS NGS Spectral Type	LGS			63
	Num LGS Subaps Across	63			
	Num NGS Subaps Across	0			
	HO Integration time	0.00113	sec		
	HO WFS CCD Read Time	0.50	frame time(s)		0.5
	HO RTC Compute Latency	0.00050	seconds		0.0005
	PnS RTC Compute Latency	0.00050	seconds		0.0005
	HOWFS Detector	CCID74			CCID74
LGS Flux	Na Column Density	3E+09	atoms/cm^2		
	Pulse Format	CW			CW
	Laser Power	50.00	Watts		50.0
	Return Calculation Basis	Measured	(Measured/Theoretical)		
	Laser-thru-LLT Transmission	0.60			0.60
HO Cent	Num Pixels per Subap Across	4			
	Pixel FoV	1.6	arcsec		1.6
	Range Gating?	NO			NO
	Intrinsic HOWFS GS diameter	0.0	arcsec	LGS	0.0
	Perfect Uplink AO?	NO			NO
	Abserrations in Uplink Beam	0.9	arcsec		0.90
	LLT Off-axis Projection Distance	0.0	m		0.0
	Use Max LGS Elongation in Calculation?	NO			
	Downlink Abserrations	0.25	arcsec		0.25
	Charge Diffusion	0.25	pixels		0.25
	ADC in HOWFS?	NO			NO
FA Tomo	Number of Laser Beacons	4			4
	LGS Beacon Height above Telescope	90	km		90
	LGS Asternism Radius	0.17	arcmin		0.17
	Single Laser Backroj FA Reduction Factor	0.8			0.8
Na H	Vertical Velocity of Na Layer	30.0	m/s		
Fit	Physical Actuator Pitch	0.0035	m		0.004
Alias	Use Anti-aliasing in HOWFS?	NO			NO
	Aliasing Reduction Factor	0.67			
Stroke	Number of Woofer Actuators Across Pupil	20			20
	Number of Tweeter Actuators Across Pupil	64			64
	Woofer Peak-to-Valley Stroke	4.0	microns		4.0
	Tweeter Peak-to-Valley Stroke	1.3	microns		1.3
	Woofer Interactor Stroke	1.2	microns		1.20
	Tweeter Interactor Stroke	0.5	microns		0.50
	Woofer Conjugate Height	0.0	meters		0.0
	Tweeter Conjugate Height	0.0	meters		0.0
	Static Surface Errors to be Corrected	1.0	microns		1.0
Go-To	Science Mode	MOAO	(SCAO/MOAO/MCAO)		MOAO
Dig	Number of Controller Bits	16	bits		16
TT Flux	TT Guide Star Brightness	1.0	mV		
	TT NGS Spectral Type	M		M	
	Subaperture Shape	circular	(circular/square)		
	Num TT Sensors Used for TT	2			2
	Num TTFA Sensors Used for TT	1			1
	Num 3x3 Sensors Used for TT	0			0
	Num HOWFS Used for TT	0			0
	TT Integration Time	0.0049	sec		
	TT Compensation Mode	Indep PnS	(SCAO/MOAO/MCAO/MOAO Point and)	Indep PnS	
	TT Detector	H2RG	(Pyramid/SH)	H2RG	
TT Meas	TT Sensor Type	SH		SH	
	TT Star Sharpened by AO?	YES		YES	
	Assume Fermina TT Sharpening?	NO			
	ADC in TT sensor?	NO			NO
	Num TT Pixels Across Subap	2			
	TT Binning Factor	1			1
	TT Pixel FoV	0.02	arcsec		0.015
	Intrinsic TT GS diameter	0.0	arcsec	0.0	
TWFS Flux	TWFS Guide Star Brightness	10.0	mV		
	TWFS NGS Spectral Type	M		M	
	Num TWFS Subaps Across	5			5
	Num TWFS Pixels Across Subap	8			8
	TWFS Integration Time	2.8200	sec		
	TWFS Compensation Mode	SCAO	(SCAO/MOAO/MCAO)	SCAO	
	TWFS Pixel FoV	0.40	arcsec		0.4
	TWFS Detector	CCD39			CCD39
Bandwidth	Kappa	1.0			1.0
	HO Servo Decimation Factor	20			20
	TT Servo Decimation Factor	20			20
	Telescope Input TT Reduction Factor	0.25			0.3
	LGS Focus Sensor	TWFS	(TWFS/TT)		TWFS
Aniso	Optimize LGS Off-pointing	NO			
	HO GS to Target for Sci Aniso WFE	1.0	arcsec		1.0
	HO GS to TT GS for TT Aniso WFE	41.1	arcsec		
	TT GS to Target (for TT Anisoplanatism)	42.1	arcsec		
	TWFS GS to Target (for Truth Anisoplanatism)	42.1	arcsec		
CA	CA Rejection Factor	20			20
Atm Dispersion	Science ADC?	YES			YES
	Science Dispersion Correction Factor	20			
Cal	Instrument	DAVINCI		DAVINCI	
	Uncorrectable AO System Aberrations	33	nm		33
	Dynamic WFS Zero-point Calibration Error	25	nm		25
	Leaky Integrator Zero-point Calibration Error	10	nm		10
	DM-to-lenslet Misregistration Errors	25	nm		25
	DM-to-lenslet Scale Errors	10	nm		10
Margins	High Order Wavefront Error Margin	45	nm		45
	Tip-tilt Error Margin	2.0	mas		2.0
Sky Coverage	TT Star Density Model	Spagna			
	Required Sky Coverage Fraction	30%			30%
	TWFS Star Density Model	Bachall			
	Required TWFS Sky Coverage Fraction	30%			
	Galactic Latitude, B	60	deg		60
Science Filter	Primary Science Filter	K			K
	Max Science Exposure Time	1800	sec		1800
Worksheet	Parameter	Current Parameter Value	Units	Galaxy Assembly	NGAO LGS

Table 5. Architectural decisions and key parameters for NGAO for the Galaxy Assembly Science Case.

5 Detailed Error Budget for Galaxy Assembly Key Science Case

5.1 Science Path Wavefront Error Budget

Keck Wavefront Error Budget Summary				Version 2.0		Science Band															
Mode: NGAO LGS						u'	g'	r'	i'	Z	Y	J	H	K							
Instrument: DAVINCI						λ (μm)	0.36	0.47	0.62	0.75	0.88	1.03	1.25	1.64	2.20						
Sci. Observation: Galaxy Assembly						$\delta\lambda$ (μm)	0.06	0.14	0.14	0.15	0.12	0.12	0.16	0.29	0.34						
						λ/D (mas)	6.7	8.8	11.6	14.1	16.6	19.4	23.5	30.8	41.4						
Science High-order Errors (LGS Mode)				Wavefront Error (rms)	Parameter	Strehl Ratio (%)															
Atmospheric Fitting Error				50 nm	60 Subaps																
Bandwidth Error				63 nm	46 Hz (-3db)																
High-order Measurement Error				69 nm	50 W																
LGS Tomography Error				37 nm	4 sci beacon(s)																
Asternism Deformation Error				16 nm	0.50 m LLT																
Chromatic Error				1 nm	Upper limit																
Dispersion Displacement Error				1 nm	Estimate																
Multispectral Error				25 nm	30 zen; sci wav																
Scintillation Error				12 nm	0.34 Scint index at 0.5um																
WFS Scintillation Error				10 nm	Allocation																
				117 nm																	
Uncorrectable Static Telescope Aberrations				43 nm	64 Acts Across Pupil																
Uncorrectable Dynamic Telescope Aberrations				38 nm	Dekens Ph.D																
Static WFS Zero-point Calibration Error				25 nm	Allocation																
Dynamic WFS Zero-point Calibration Error				25 nm	Allocation																
Leaky Integrator Zero-point Calibration Error				10 nm	Allocation																
Stale Reconstructor Error				15 nm	Allocation																
Go-to Control Errors				30 nm	Allocation																
Residual Na Layer Focus Change				39 nm	30 m/s Na layer vel																
DM Finite Stroke Errors				6 nm	5.3 μm P-P stroke																
DM Hysteresis				13 nm	from TMT model																
High-Order Aliasing Error				17 nm	60 Subaps																
DM Drive Digitization				1 nm	16 bits																
Uncorrectable AO System Aberrations				33 nm	Allocation																
Uncorrectable Instrument Aberrations				30 nm	DAVINCI																
DM-to-lenslet Misregistration				15 nm	Allocation																
DM-to-lenslet Pupil Scale Error				15 nm	Allocation																
				101 nm																	
Angular Anisoplanatism Error				16 nm	1.0 arcsec																
HO Wavefront Error Margin				45 nm	Allocation																
Total High Order Wavefront Error				154 nm	162 nm	High Order Strehl	0.00	0.01	0.07	0.16	0.27	0.39	0.53	0.69	0.81						
Science Tip/Tilt Errors				Angular Error (rms)	Equivalent WFE (rms)	Parameter	Strehl ratios (%)														
Sci Filter																					
Tilt Measurement Error (one-axis)				1.92 mas	33 nm	19.0 mag (mV)															
Tilt Bandwidth Error (one-axis)				1.30 mas	22 nm	9.5 Hz (-3db)															
Tilt Anisoplanatism Error (one-axis)				3.23 mas	55 nm	42.0 arcsec from sci															
Residual Centroid Anisoplanatism				0.55 mas	9 nm	20 x reduction															
Residual Atmospheric Dispersion				0.12 mas	2 nm	20 x reduction															
Induced Plate Scale Deformations				0.00 mas	0 nm	0 m con height															
Non-Common-Path Tip-Tilt Errors				1.60 mas	27 nm	3.2 mas Allocation															
Residual Telescope Pointing Jitter (one-axis)				1.22 mas	21 nm	29 Hz input disturbance															
TT Error Margin				2.00 mas	195 nm	Allocation															
Total Tip/Tilt Error (one-axis)				4.9 mas	91 nm	Tip/Tilt Strehl	0.27	0.39	0.53	0.62	0.70	0.76	0.82	0.89	0.94						
Total Effective Wavefront Error				184 nm	Total Strehl (%)	0.00	0.00	0.04	0.10	0.19	0.29	0.43	0.61	0.76							
						FWHM (mas)	8.3	10.1	12.6	14.9	17.3	20.0	24.1	31.2	41.7						
						Spaxel / Aperture Diameter (mas)	41	83	34	70	90	120	240	650	800	40					
Ensquared Energy				K	Square	0.45	0.78	0.36	0.74	0.80	0.82	0.85	0.91	0.91	0.50						
					Seeing-Limited	0.01	0.02	0.00	0.02	0.03	0.05	0.20	0.79	0.90							
Sky Coverage				Galactic Latitude	60 deg																
Corresponding Sky Coverage				30%	This fraction of sky can be corrected to the Total Effective WFE shown																
Assumptions / Parameters																					
Atmospheric / Observing Parameters				System Parameters				LO WFS Magnitudes				Derived Values									
Zenith Angle	30 deg	LGS Asterism Radius	0.17 arcmin	20.0	19.3	18.4	17.5	17.2	16.8	16.3	15.2	14.1									
r0	0.147 m	LGS Power	50 W																		
theta0_off	2.145 arcsec	BYO Transmission	0.60																		
Wind Speed	10.97 m/s	HO WFS Transmission	0.38																		
Outer Scale	50 m	HO WFS Type	SH using	CCID74																	
Sodium Abundance	$3 \times 10^9 \text{ cm}^{-2}$	HO WFS Noise	1.7 e- rms																		
AO Modes of Operation				HO WFS Anti-aliasing				LO WFS Rate				LO WFS Rate									
Science AO Mode	MOAO	LO WFS Transmission	0.29																		
LOWFS AO Mode	Indep PnS	LO WFS Type	SH using	H2RG																	
				LO WFS Noise				Detected PDE/subap/exp				152									
				LO WFS Star Type																	
				Max TT Rejection Bandwidth																	
TT	2	Observation Parameters																			
TIFA	1	Max Exposure Time				1800 sec															
3x3	0																				
HOWFS	0																				

Table 6. Galaxy Assembly Case Wavefront and Ensquared Energy Budget

6 LGS Mode operation with 5 x 5 subaperture NGS WFS TWFS mode

6.1 Describe the mode of operation

There are two NGAO modes of operation that require use of the visible-light NGS WFS in a 5x5 subaperture pupil sampling mode: Pupil Fixed mode operation (typical of exoplanet searches and characterization) and in Image Fixed mode when the availability of field NGS for LO WFS sensing of TT and blind mode sensing is not favorable compared to use of the science target itself for both TT and blind mode information.

6.2 Performance Estimate

In theory, it may be possible to combine information from the NGS WFS in TWFS mode with information from the LO WFS, to further optimize performance, but this will not be investigated here. Instead, we would like to understand the TT performance (only) of the NGS WFS in TWFS mode, as a function of science target brightness, and more specifically we're interested in knowing how the red-wavelength NGS WFS cutoff choice affects performance in the NGS WFS TWFS mode. The results of just such a trade study are shown in Figure 4.

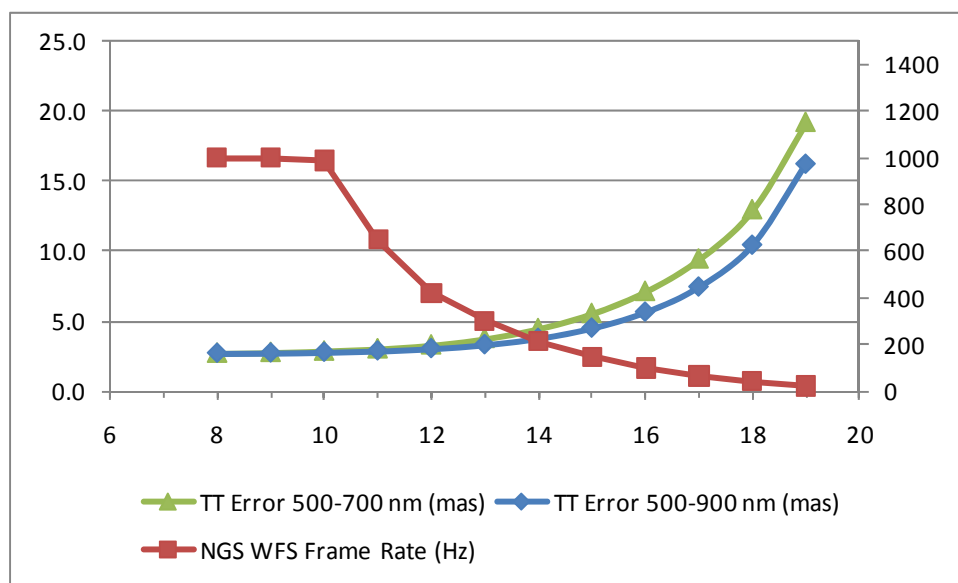


Figure 1. Performance of the NGAO NGS WFS for TT measurement, when operating in 5x5 subaperture TWFS mode, for NGS passband approximately 500 – 900 nm, compared to passband approximately 500 – 700 nm. These curves are optimized for best TT performance, and do not include the degradation of TWFS sensing of the laser tomography blind modes as the NGS WFS frame rate is slowed. The indicated optimal NGS WFS frame rate corresponds to the 500 – 900 nm passband case.

In generating Figure 1, we assume that the NGS WFS frame rate is optimized to provide the best TT measurement, without regard to the potential impact on its ability to accurately measure the laser tomography blind modes. If we assume that the need for accurate blind mode measurement requires us to operate the NGS WFS in TWFS mode no slower than 200 Hz (an admittedly arbitrary number), the quality of NGS WFS TT sensing breaks down considerable faster, as shown in Figure 2.

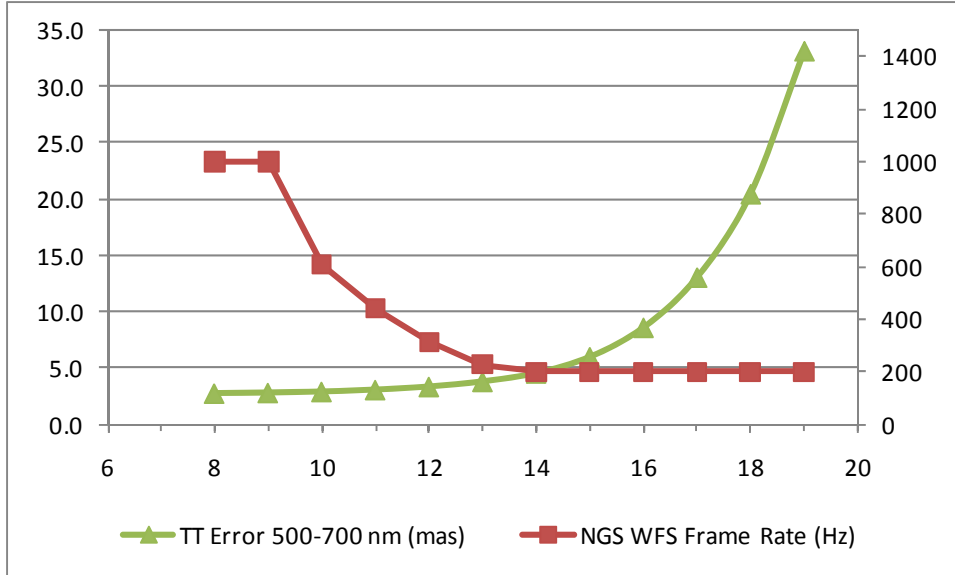


Figure 2 Performance of the NGAO NGS WFS for TT measurement, when operating in 5x5 subaperture TWFS mode, for NGS passband approximately 500 – 700 nm, with a minimum frame rate limit of 200 Hz. This may be more indicative of TT operation when the NGS WFS is required to read out relatively fast to maintain good blind mode measurement.

7 Trade Studies

7.1 Performance vs. Seeing

NGAO will have to operate in a wide range of natural seeing conditions, so it is interesting to understand the sensitivity of performance to changes in the Fried parameter, r_0 . This is shown for the Galaxy Assembly Science Case in Figure 3.

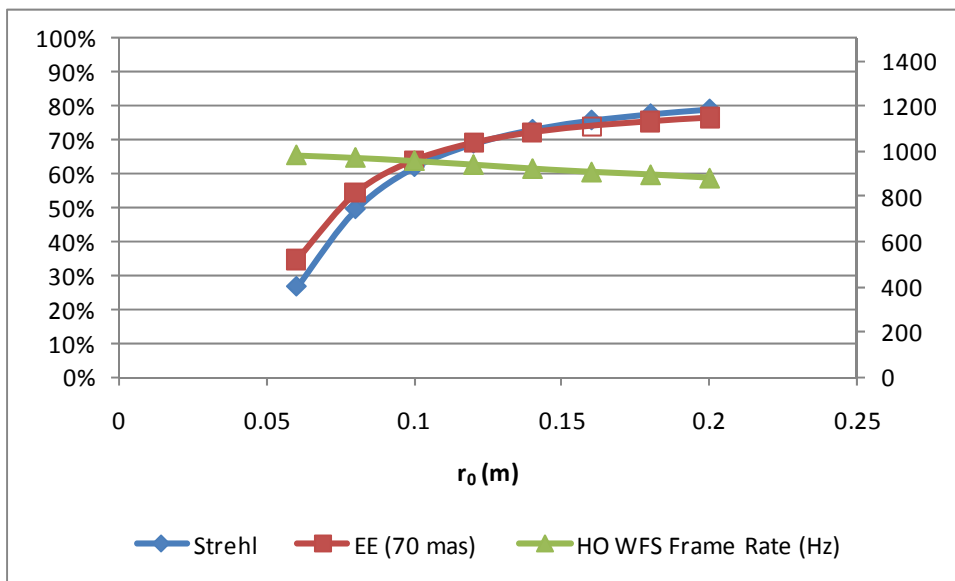


Figure 3. K-band performance for the Galaxy Assembly Science Case as a function of r_0 at 0.5 microns.

7.2 Performance vs. Wind Speed

The 3-dimensional wind profile of the atmosphere above Mauna Kea can vary dramatically. Although we adopt as our median a value of 9.5 m/s, we would like to understand how performance degrades with increasing turbulence-weighted wind speed, and how it might improve under calmer conditions. Figure 4 demonstrates the sensitivity of performance, which is rather benign for the Galaxy Assembly Science Case, even for wind speeds treble our median assumption. As the wind speed is increased, the corresponding HO WFS frame rate increases (and recall, in the current KAON 721 model, this also simultaneously increases the HO WFS CCD pixel readout rate.) For a fixed pixel read rate, NGAO will have somewhat more performance sensitivity to high wind speeds, as the rejection bandwidth of atmospheric turbulence may not be able to keep up so optimally with increasing frame rate.

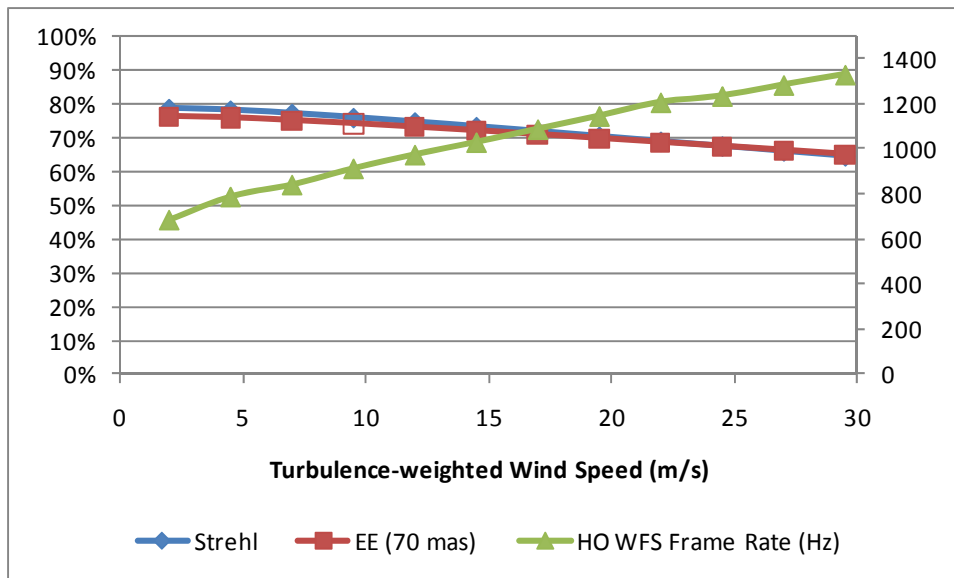


Figure 4. K-band performance for the Galaxy Assembly Science Case as a function of turbulence-weighted wind speed. The open marker indicates the median 9.5 m/s wind speed condition.

7.3 Performance vs. Laser Return

Experience with the first-generation sodium D2-line resonant excitation LGS at Lick, Keck, and Palomar Observatories has shown that measured sodium photoflux can vary widely due to be sodium abundance fluctuations (see §7.4), but also because of variability in laser power and degradations in optical transmission in beam transfer uplink or AO system downlink optical systems.

We are interested in understanding the sensitivity of NGAO to variations in the expected sodium return photoflux. The results of two trade studies are shown in Figure 5 and Figure 6. In the first of these, we consider the impact of different levels of laser (spigot) power in absolute terms (assuming our usual “SOR-like” laser return) while in the second, we describe it as a percentage of the expected laser return

(typically 55 photodetection events (PDE) / exposure time / subaperture, or $57 / (.1825^2) / 0.0011 = 1.55 \times 10^6$ PDE/sec/m² or ~ 155 PDE/sec/cm², for each of the 12.5W (spigot) fixed asterism LGS¹⁴).

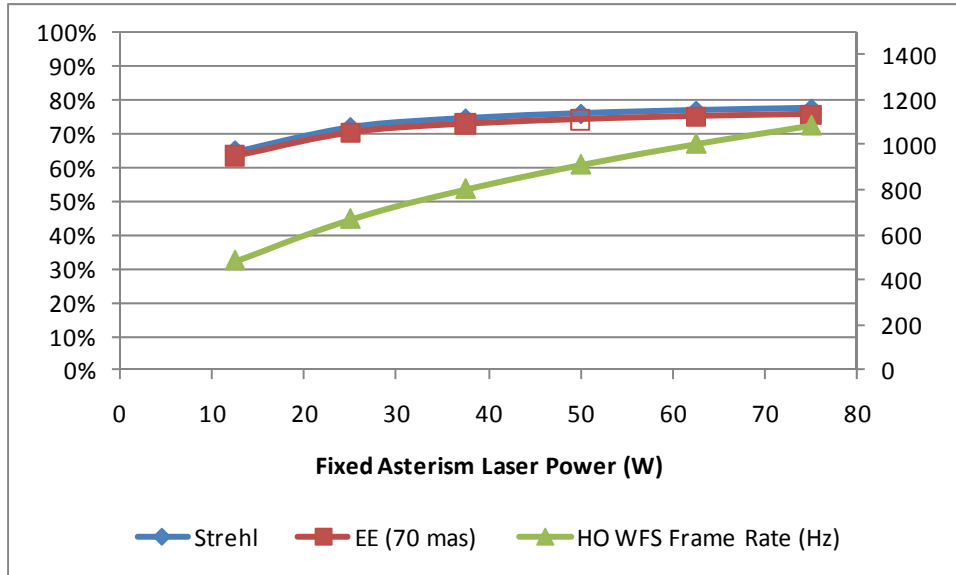


Figure 5 K-band performance for the Galaxy Assembly Science Case as a function of fixed asterism laser power, holding patrolling asterism laser power constant at 25W (e.g. 3 x 8.33 W each.) The open marker indicates the baseline 50W of fixed asterism laser power (spigot).

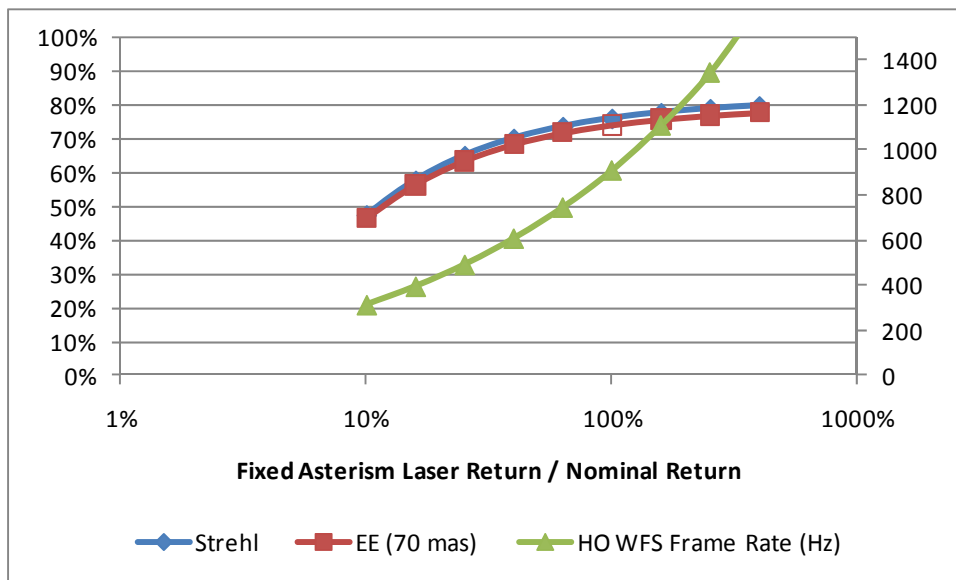


Figure 6. K-band performance for the Galaxy Assembly Science Case as a function of fixed asterism laser return, relative to the expected return using our baseline conditions model (e.g. 3 x 10⁹ atoms/cm² sodium density, SOR-laser-like return,

¹⁴ We assume 75 ph/sec/cm²/W return from a 3 x 10⁹ atoms/cm² sodium layer (itself from Denman’s reported 150 ph/sec/cm² from Albuquerque with 4 x 10⁹ atoms/cm² – see KAON 721), with 50W/4*.6 (BTO)*.88 (Atm) = 6.6 W per beacon delivered to mesosphere (495 ph/sec/cm² at mesosphere), followed by T=0.35, QE=0.85 on the downlink results in about 155 ph/sec/cm² detected by the WFS.

delivered and return transmission assumptions, etc.), holding patrolling asterism laser power constant at 25W (e.g 3 x 8.33 W each.) The robustness of NGAO to less-than-expected laser return is clear for this science case.

7.4 Seeing, Wind Speed, and Sodium Abundance Monte Carlo Results

Although practically useful in understanding the sensitivities of NGAO performance to both seeing and turbulence-weighted wind speed variations, in practice NGAO will see on any given night seeing and wind speed values that are random variables drawn from some statistical distributions. In fact, there exists considerable detail on the statistics of these parameters at Mauna Kea. For my current purpose, however, an approximate form of these distributions will suffice to indicate the typical distribution of performance we might expect from a large number of observing nights. To quickly model this, I can assume that both r_0 and wind speed are drawn from Gaussian probability distributions. Following the technique in 'Numerical Recipes in C, 2nd Ed', page 289, we generated in Excel draws of the form:

	Mean	Standard Deviation, σ
r_0 at 0.5 microns	0.16 m	0.025 m
Wind speed	9.5 m/s	4 m/s

where the distribution standard deviations, σ , are coarse estimates based on KAON 303. (A detailed determination of σ is unlikely to improve these results, as I contend we are within the uncertainty level of the model¹⁵.)

The results of 252 random draws (and frame rate optimizations) from this joint probably distribution is shown in Figure 7, for the case of mesospheric sodium abundance held constant at the below-median level of 3×10^9 atoms/cm². Note, unlike the current Keck 2 AO system, NGAO is seen to vary rarely deliver performance less than about 60% K-band Strehl ratio. Moreover, the system is expected to deliver K-Strehls within a few percent of 78%, across varying different atmospheric conditions, a rather remarkable qualitative difference over current AO that we expect to improve both photometric accuracy and astrometric precision.

¹⁵ For these Gaussian distributions, we also truncate the distribution to avoid negative values. Although not strictly valid, in practice it has little effect on the results shown here (e.g. we're not primarily interested in these rare outlier events.)

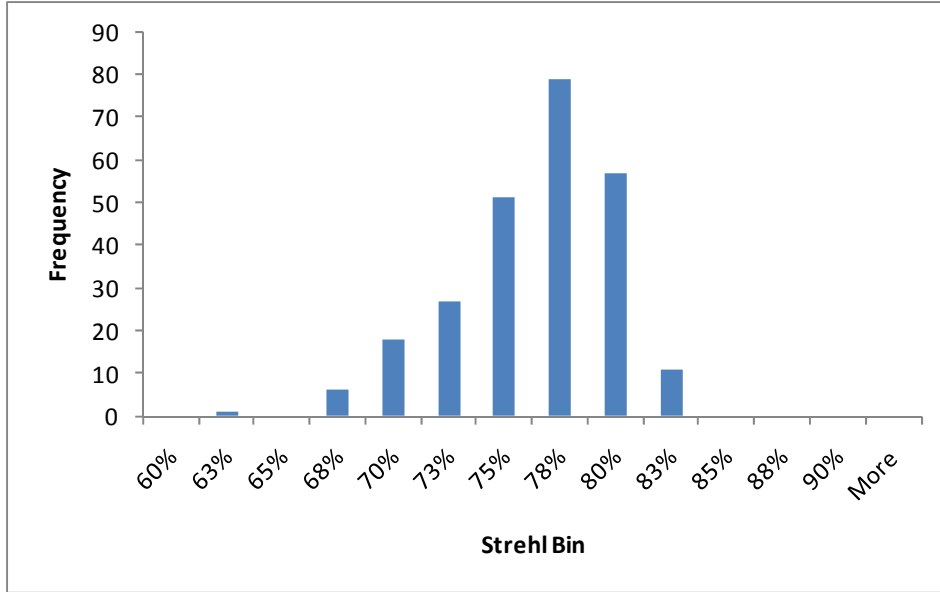


Figure 7. Predicted performance distribution for NGAO based upon 252 r_0 and wind speed draws, holding sodium abundance constant at $3e9$ atoms/cm², for the Galaxy Assembly Science Case.

Because sodium abundance can also vary, we repeated this random draw experiment, adding it as a third joint random variable:

	Mean	Standard Deviation, σ
Sodium abundance	3.6×10^9 atoms/cm ²	1.0×10^9 atoms/cm ²

Where the mean is taken from KAON 416 and the standard deviation estimated from the fact that experience has shown the large majority (~90%) of time density is thought to be between 1.6×10^9 and 5.6×10^9 atoms/cm² (e.g. $\pm 2\sigma$). This result, for 394 random draws, is shown in Figure 8. Not surprisingly, this histogram is shifted to somewhat higher performance compared to our earlier sub-median sodium abundance curve. Because sometimes the abundance can fall, even in conjunction with good seeing and slow winds, the (relatively) poorer performance tail is now seen to be extended, though still almost always above 60% K-Strehl.

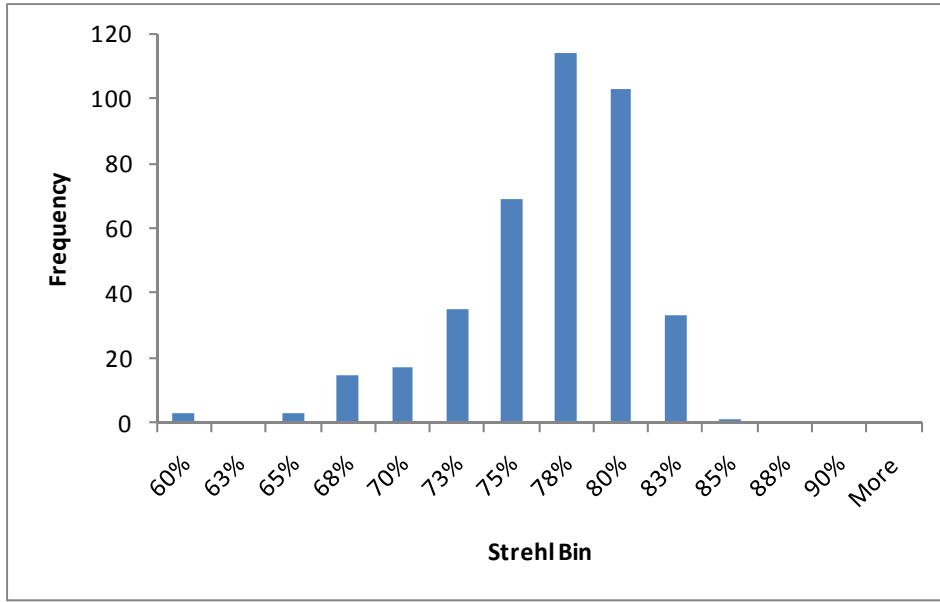


Figure 8. Predicted performance distribution for NGAO based upon 394 r_0 , wind speed, and sodium abundance draws for the Galaxy Assembly Science Case.

To better appreciate the advantage of NGAO over current Keck 2 AO, we repeated the experiment described in Figure 8 with a mirror experiment, using the same parameter distributions, for our model of the Keck 2 AO system (previously validated as described in KAON 461). This result is shown in Figure 9. The first obvious benefit of NGAO is an approximately 3x improvement in K-band Strehl ratio over current Keck 2 AO, which directly improves telescope sensitivity for background-limited imaging. The difference in results distribution width is also quite striking, particularly if one considers the *relative* stability of the predicted results, with NGAO showing perhaps $\pm 4\%$ variation around a 78% peak ($\pm 5\%$ relative), while the Keck 2 AO result shows $\pm 10\%$ around a 30% median, which is more like $\pm 33\%$ relative variation.

The skewness of these distributions is also worth noting. For Keck 2 AO, the longer tail is toward good performance, so it is more likely that an observer will have heard of someone at some time having a particularly good result with Keck 2 AO, but the median performance, they're average experience with AO, tends to fall short of this. For NGAO, on the other hand, we expect the user experience to be more often consistent with the maximum capability of the system. The occasional unfortunate night for an NGAO observer will doubtless draw heartfelt condolences from their colleagues.

More practically, NGAO instrument development will also benefit from this tendency to deliver more predictable image quality, perhaps by reducing the number of configurations, such as plate scales, that is typically necessary when delivered performance is widely variable.

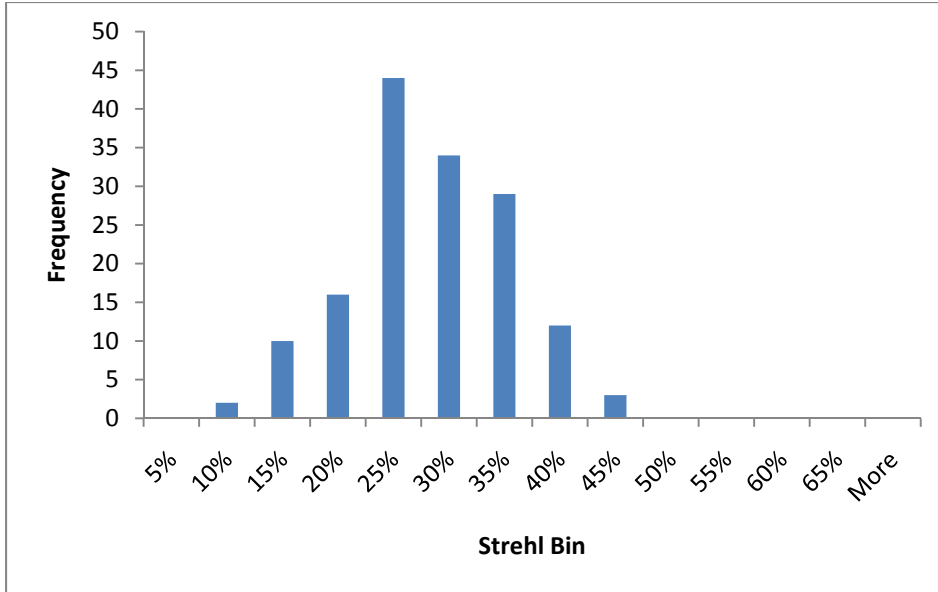


Figure 9 Predicted performance distribution for the current Keck 2 AO system based upon 150 r_0 , wind speed, and sodium abundance draws for the Galaxy Assembly Science Case. Note the change in Strehl Bin scale compared to the NGAO predictions.

7.5 Performance vs. Sky Fraction

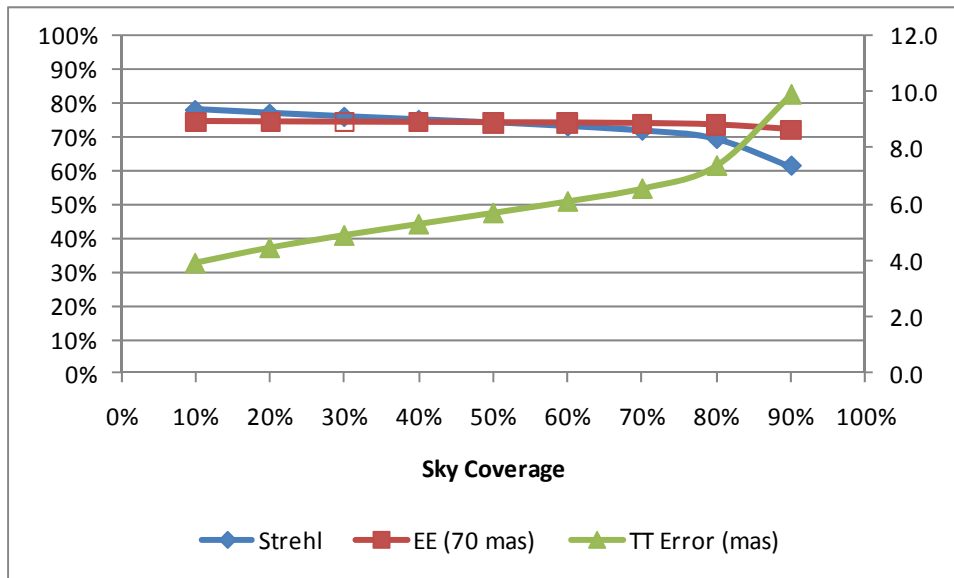


Figure 10. K-band performance for the Galaxy Assembly Science Case as a function of sky coverage percentage, representing the likely of finding three NGS of sufficient brightness to achieved the indicated performance, within the FoR of the LO WFS. The residual TT error varies from about 4 mas to about 9 mas as the sky coverage fraction is increased.

7.6 Performance vs. LO WFS Passband

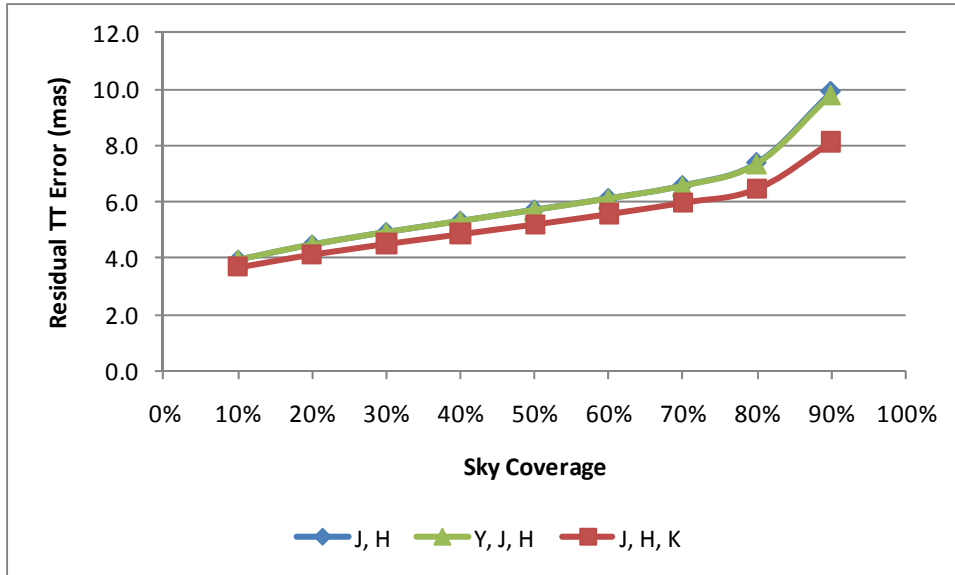


Figure 11. Residual TT error for the Galaxy Assembly Science Case as a function of sky coverage percentage, for three different choices of LO WFS passband. Inclusion of the design-complicating K-band is comparable to the uncertainty in our models, excepting perhaps at the highest sky fraction, where the advantage of including K-band would probably be real. Note, KAON 721 does not currently account for inter-filter-band sky emissions. Thus, these results should be considered for e.g. J + H, not the full range J through H. As such, the relative advantage of including K-band is probably overstated here.

7.7 Performance vs. Spaxel Sampling

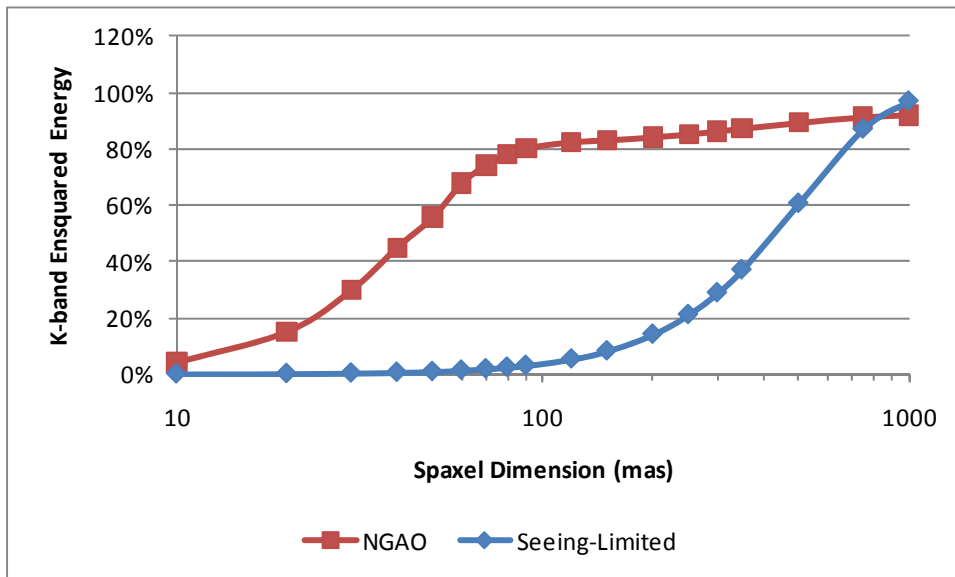


Figure 12. K-band Ensquared Energy vs. Spaxel Dimension for the Galaxy Assembly Science Case for NGAO correction and, for comparison, a seeing-limited PSF in median seeing conditions. (The relative transmission loss of NGAO compared to a Nasmyth-mounted seeing-limited instrument is not represented here – these curves reflect PSF shape only.)

Appendix A: System Compliance Matrix

XXX This matrix is completed and posted to the TWiki. Should it or parts of it be included here? XXX

Appendix B: Wavefront Error Budget Spreadsheet v2.0

XXX These are only snippets of text – will be cleaned up later XXX

KAON 721 consists of a Microsoft Excel spreadsheet encoding the following for the purposes of developing adaptive optics system error budgets and evaluating as-built adaptive optics system performance:

- AO system architectures and design choices
- Atmospheric turbulence models
- Telescope parameters and as-built optical performance metrics
- Astronomical detector properties, such as quantum efficiency, dark current, and read noise
- Numerous adaptive optics error budget terms, specific to any of several distinct AO system architectures (e.g. SCAO, MCAO, MOAO) for both NGS and LGS guide star modes
- Atmospheric dispersion
- Calibration and systematic error terms, such as thermally induced non-common-path flexure
- Several astronomical stellar density models for the evaluation of AO sky coverage

The spreadsheet also computes ensquared energy fractions using a core/halo model for the point spread function, and calculates sky coverage estimates for tip tilt guide stars employed in laser guide star architectures from common star density models.

XXX Include a paragraph on validation activities here XXX

The terms in the previously presented tables are largely self-explanatory, although their quantitative implementation requires reference to KAON 721 itself. All the same, a few items in Table 5 are worthy of additional explanation here:

- HO Flux, Number of Subapertures Across: NGAO has high-order wavefront sensors designed to sample the telescope pupil with ~60 subapertures across the 10.949 m maximum diameter. Our WFS's, however, are designed for 63 x 63 subaperture format (e.g. oversizing the pupil somewhat) to handle known pupil nutation in the Keck telescopes. See Keck Drawing 1410-CM0010 for more detail.
- HO Flux, HO WFS CCD Read Time is currently given as a fraction of the HO WFS frame rate, which is typically an optimization variable. In the future, this will be replaced with an amplifier dwell time or equivalent parameter to specify the detector read time.
- LGS Flux, Na Column Density of $3e9$ atoms/cm² is below median density (approximately 25th percentile). See Figure XXX for a trade study of performance vs. sodium density.
- TT Flux, TT Compensation Mode is a complex choice that supports traditional single-conjugate AO correction, MCAO, single-LGS MOAO correction, and multiple patrolling LGS (aka 'Point and Shoot') architectures. Changes to this parameter must be carefully understood by the KAON 721 user.

- Atm Dispersion, Science Dispersion Corrector Factor uses a crude multiplicative (divisive, actually) factor to estimate the residual performance, if a science ADC is used. In the future, KAON 721 will allow for definition of more realistic, design-informed residual dispersion.
- Margins (e.g. performance margins) are held apart from physical error terms and constitute the difference between use of KAON 721 as an error budget (including margins) and as a performance prediction or system diagnostic tool (assuming margins are not invoked.)

Appendix C: Detailed Error Budgets

XXX This is only a draft example of the screen captures for the ExoPlanets and Gal Center. These will be replaced in the final draft XXX

Input Summary

Worksheet	Parameter	Current Parameter Value	Units	Io	Vesta	Exo Jup NGS	Mira Vars	Faint NGS	Gal Cen	Gal Cen Spectra	Exo-planets	T Tauri	Transients	Astrometry	Debris Disks	Minor Planets	Galaxy Assembly	Nearby AGN	NGAO NGS	NGAO LGS		
Telescope	Name	Keck																	Keck	Keck		
Atm	Declination			-10	-10				-30	-30								-12		20	20	
	Zenith Angle	50.0	deg	Dec	Dec	30	30	10	Dec	Dec	30	30	10	10	10	10	Dec	30	30	50	50	
	Cr2(h) Model	Mauna Kea Ridge																	Mauna Kea Ridge	Kea Ridge	0.160	0.160
	IO at Zenith	0.160	m																		9.5	9.5
	Wind speed	9.5	m/s																		50	50
	Outer Scale	50	m																			
HO Flux	Guide Star Spectral Type	LGS (NGS/LGS)		NGS	NGS	NGS	NGS	NGS	LGS	LGS	LGS	LGS	LGS	LGS	LGS	LGS	LGS	LGS	LGS	LGS		
	Guide Star Brightness	LGS mV		5.0	8.0	0.0	10.0	16.0														
	HOWFS NGS Spectral Type	LGS		G	G	M	M	K														
	Num LGS Subapcs Across	63																				63
	Num NGS Subapcs Across	0																				
	HO Integration time	0.00104	sec																			0.5
	HO WFS CCD Read Time	0.30	frame time(s)																			0.0005
	HO RTC Compute Latency	0.00050	seconds																			0.0005
	PrS RTC Compute Latency	0.00050	seconds																			0.0005
	HOWFS Detector	CCID74																				CCID74
LGS Flux	Na Column Density	3E+09	atoms/cm^2																			
	Pulse Format	CW																				CW
	Laser Power	50.00	Watts																			50.0
	Return Calculation Basis	Measured	(Measured/Theoretical)	Measured																		
	Laser thru-LT Transmission	0.60																				0.60
HO Cent	Num Pixels per Subap Across	4																				4
	Pixel Fov	1.6	arcsec																			1.6
	Range Gating?	NO																				NO
	Intrinsic HOWFS GS diameter	0.0	arcsec	1.1	0.3	0.0	0.0	0.0	LGS	LGS	LGS	LGS	LGS	LGS	LGS	LGS	LGS	LGS	LGS	LGS		0.0
	Perfect Uplink AO?	NO																				NO
	Abserrations in Uplink Beam	0.9	arcsec																			0.90
	LLT Off-axis Projection Distance	0.0	m																			0.0
	Use Max LGS Elongation in Calculation?	NO																				NO
	Downlink Abserrations	0.25	arcsec																			0.25
	Charge Diffusion	0.25	pixels																			0.25
	ADC in HOWFS?	NO																				NO
FA Tomo	Number of Laser Beacons	4																				4
	LGS Beacon Height above Telescope	90	km																			90
	LGS Asternm Radius	0.17	arcmin																			0.17
	Single Laser Backlog FA Reduction Factor	0.8																				0.8
Na H	Vertical Velocity of Na Layer	30.0	m/s																			30.0
Fit	Physical Actuator Pitch	0.0035	m																			0.004
Alias	Use Anti-aliasing in HOWFS?	NO																				YES
	Aliasing Reduction Factor	0.67																				0.67
Stroke	Number of Woofer Actuators Across Pupil	20																				20
	Number of Tweeter Actuators Across Pupil	64																				64
	Woofer Peak-to-Valley Stroke	4.0	microns																			4.0
	Tweeter Peak-to-Valley Stroke	1.3	microns																			1.3
	Woofer Interactuator Stroke	1.2	microns																			1.20
	Tweeter Interactuator Stroke	0.5	microns																			0.50
	Woofer Conjugate Height	0.0	meters																			0.0
	Tweeter Conjugate Height	0.0	meters																			0.0
	Static Surface Errors to be Corrected	1.0	microns																			1.0
Go-To	Science Mode	MOAO	(SCAO/MOAO/MCAO)																			SCAO
Dig	Number of Controller Bits	16	bits																			16
TT Flux	TT Guide Star Brightness	12.7	mV	5.0	8.0	LGS	10.0	16.0	12.2	12.2	18.3	18.0	17.0	19.0	16.0							
	TT NGS Spectral Type	IRS7		G	G	M	M	K	IRS7	IRS7	M	M	M	M	M	M	M	M	M	M		
	Subapcs Shape	circular	(circular/square)	circular																		0
	Num TT Sensors Used for TT	2																				0
	Num TIFA Sensors Used for TT	1																				0
	Num 3x3 Sensors Used for TT	0																				0
	Num HOWFS Used for TT	0																				1
	TT Integration Time	0.0009	sec																			
	TT Compensation Mode	Indep PrS	(SCAO/MOAO/MCAO/MOAO Point and Shoot,Indep PrS)																			Indep PrS
	TT Detector	H2RG																				H2RG
TT Meas	TT Sensor Type	SH	(Pyramid/SH)																			SH
	TT Star Sharpened by AO?	YES																				NO
	Assume Fermina TT Sharpening?	NO																				NO
	ADC in TT sensor?	NO																				NO
	Num TT Pixels Across Subap	2																				2
	TT Binning Factor	1																				1
	TT Pixel Fov	0.02	arcsec	1.1	0.3	0.0	0.0	0.0	0.0	0.0	0.0	0.0	0.0	0.0	0.0	0.0	0.0	0.0	0.0	0.0		0.015
	Intrinsic TT GS diameter	0.0	arcsec																			
TWFS Flux	TWFS Guide Star Brightness	12.7	mV	0.0	0.0	0.0	0.0	0.0	12.2	12.2	18.3	18.0	17.0	21.0	16.0							
	TWFS NGS Spectral Type	K		G	G	M	M	K	K	K	M	M	M	M	M	M	M	M	M	M		
	Num TWFS Subapcs Across	5																				5
	Num TWFS Pixels Across Subap	8																				8
	TWFS Integration Time	0.0093	sec																			
	TWFS Compensation Mode	SCAO	(SCAO/MOAO/MCAO)																			SCAO
	TWFS Pixel Fov	0.40	arcsec																			0.4
	TWFS Detector	CCD39																				CCD39
Bandwidth	Kappa	1.0																				1.0
	HO Seno Decimation Factor	20																				20
	TT Seno Decimation Factor	20																				20
	Telescope Input TT Reduction Factor	0.25																				0.5
	LGS Focus Sensor	TWFS	(TWFS/TT)																			TWFS
	Optimize LGS Off-pointing	NO																				NO
Aniso	HO GS to Target for Sci Aniso WFE	1.0	arcsec	0.5	0.1	1.0	2.0	5														

Galactic Center Case

Keck Wavefront Error Budget Summary			Version 2.0		Science Band															
Mode:	NGAO LGS																			
Instrument:	DAVINCI					λ (μm)	0.36	0.47	0.62	0.75	0.88	1.03	1.25	1.64	2.20					
Sci. Observation:	Gal Cen					$\delta\lambda$ (μm)	0.06	0.14	0.14	0.15	0.12	0.12	0.16	0.29	0.34					
						λ/D (mas)	6.7	8.8	11.6	14.1	16.6	19.4	23.5	30.8	41.4					
Science High-order Errors (LGS Mode)			Wavefront Error (rms)	Parameter	Strehl Ratio (%)															
Atmospheric Fitting Error			56 nm	63 Subaps																
Bandwidth Error			91 nm	48 Hz (-3db)																
High-order Measurement Error			85 nm	50 W																
LGS Tomography Error			61 nm	4 sci beacon(s)																
Asterism Deformation Error			25 nm	0.50 m LLT																
Chromatic Error			2 nm	Upper limit																
Dispersion Displacement Error			6 nm	Estimate																
Multispectral Error			34 nm	50 zen; sci wav																
Scintillation Error		H	20 nm	0.59 Scint index at 0.5um																
WFS Scintillation Error			10 nm	Allocation																
		157 nm																		
Uncorrectable Static Telescope Aberrations			43 nm	64 Acts Across Pupil																
Uncorrectable Dynamic Telescope Aberrations			36 nm	Dekens Ph.D																
Static WFS Zero-point Calibration Error			25 nm	Allocation																
Dynamic WFS Zero-point Calibration Error			25 nm	Allocation																
Leaky Integrator Zero-point Calibration Error			10 nm	Allocation																
State Reconstructor Error			15 nm	Allocation																
Go-to Control Errors			30 nm	Allocation																
Residual Na Layer Focus Change			3 nm	30 m/s Na layer vel																
DM Finite Stroke Errors			8 nm	5.3 um P-P stroke																
DM Hysteresis			13 nm	from TMT model																
High-Order Aliasing Error			19 nm	63 Subaps																
DM Drive Digitization			1 nm	16 bits																
Uncorrectable AO System Aberrations			33 nm	Allocation																
Uncorrectable Instrument Aberrations			30 nm	DAVINCI																
DM-to-lenslet Misregistration			15 nm	Allocation																
DM-to-lenslet Pupil Scale Error			15 nm	Allocation																
		93 nm																		
Angular Anisoplanatism Error			24 nm	1.0 arcsec																
HO Wavefront Error Margin			45 nm	Allocation																
Total High Order Wavefront Error		182 nm	190 nm	High Order Strehl	0.00	0.00	0.02	0.08	0.16	0.26	0.41	0.59	0.75							
Science Tip/Tilt Errors			Angular Error (rms)	Equivalent WFE (rms)	Parameter	Strehl ratios (%)														
Tilt Measurement Error (one-axis)		Sci Filter	0.13 mas	2 nm	12.2 mag (mV)															
Tilt Bandwidth Error (one-axis)			0.21 mas	4 nm	50.0 Hz (-3db)															
Tilt Anisoplanatism Error (one-axis)			0.50 mas	9 nm	5.6 arcsec from sci															
Residual Centroid Anisoplanatism			0.64 mas	11 nm	20 x reduction															
Residual Atmospheric Dispersion		H	0.53 mas	10 nm	20 x reduction															
Induced Plate Scale Deformations			0.00 mas	0 nm	0 m conj height															
Non-Common-Path Tip-Tilt Errors			0.01 mas	0 nm	3.2 mas/Allocation															
Residual Telescope Pointing Jitter (one-axis)			0.23 mas	4 nm	29 Hz input disturbance															
TT Error Margin			2.00 mas	145 nm	Allocation															
Total Tip/Tilt Error (one-axis)			2.2 mas	42 nm	Tip/Tilt Strehl	0.64	0.76	0.84	0.89	0.92	0.94	0.96	0.97	0.99						
Total Effective Wavefront Error			194 nm	Total Strehl (%)	0.00	0.00	0.02	0.07	0.15	0.25	0.39	0.58	0.74							
				FWHM (mas)	7.1	9.1	11.8	14.3	16.8	19.6	23.7	30.9	41.5							
			Spaxel / Aperture Diameter (mas)	31	62	34	70	90	450	500	650	800	44							
Ensquared Energy		H	Square	0.33	0.57	0.38	0.59	0.60	0.74	0.76	0.80	0.83	0.50							
Sky Coverage		Galactic Latitude	0 deg																	
Corresponding Sky Coverage			7%	This fraction of sky can be corrected to the Total Effective WFE shown																

